

Comparative Studies of Grafting and Direct Syntheses of Inorganic–Organic Hybrid Mesoporous Materials

Myong H. Lim and Andreas Stein*

Department of Chemistry, University of Minnesota, 207 Pleasant St. SE,
Minneapolis, Minnesota 55455-0431

Received June 9, 1999. Revised Manuscript Received August 9, 1999

Vinyl-functionalized MCM-41 samples were prepared by either a postsynthesis grafting (PSG) process or a direct co-condensation synthesis. The structures, stabilities, and reactivities of products from both methods were compared. The mesoscopic order of the hexagonal pore structure of vinyl-grafted MCM-41 (v-gr-MCM-41) resembled that of the MCM-41 host. On the basis of powder X-ray diffraction (PXRD), X-ray photoelectron spectroscopy (XPS), and bromination kinetics data, the vinyl groups appeared to be nonuniformly distributed in v-gr-MCM-41 prepared by the present PSG process, with a large proportion of vinyl groups on the external surface of the crystallites or inside channels but near the channel openings. The mesoscopic order of products from the direct synthesis (v-MCM-41) depended on the type of alkoxysilane precursor used and on the ratio of vinylsiloxane to alkoxysilane in the reaction mixture. The vinyl groups appeared to be more uniformly distributed in v-MCM-41. Vinyl-grafted MCM-41 exhibited greater hydrothermal stability than unmodified MCM-41 and was capable of absorbing nonpolar solvents from aqueous mixtures or emulsions.

Introduction

Various methods of functionalizing the surfaces of periodic mesoporous materials with organic groups have been investigated in recent years because surface modification permits tailoring of the surface properties for numerous potential applications including catalysis, ion exchange, encapsulation of transition-metal complexes or semiconductor clusters, chemical sensing, and nanomaterial fabrication.^{1–7} As a support for organic functional groups, hexagonally ordered MCM-41^{8,9} is particularly interesting due to its high surface area and uniform pore size distribution in the mesopore size range. Hybrid mesoporous sieves take advantage of the properties of the inorganic support, as well as of the organic surface groups. The polymeric silica framework of MCM-41 provides structural order, as well as thermal and mechanical stability, whereas organic species incorporated into the inorganic phases permit versatile control of interfacial and bulk materials characteristics,

such as porosity, hydrophobicity, and optical, electrical, or magnetic properties.

Organic functionalization of the internal surface of a MCM-41 host can be achieved either by covalently grafting various organic species onto the channel walls^{4,9–13} or by incorporating functionalities directly during the preparation.^{1–3,14–21} The first approach, a postsynthesis grafting (PSG) process, has been widely employed to anchor specific organic groups onto surface silanols of diverse silica supports. Typically, organochlorosilanes or organoalkoxysilanes are used as precursors for the surface modification. In this method, the host materials should be dried carefully prior to adding precursors to avoid self-condensation of precursors in the presence of H₂O. Control over the concentration and distribution of organic moieties in MCM-41 by the PSG method is constrained by the number of surface silanol

- (1) Lim, M. H.; Blanford, C. F.; Stein, A. *J. Am. Chem. Soc.* **1997**, *119*, 4090–4091.
- (2) Lim, M. H.; Blanford, C. F.; Stein, A. *Chem. Mater.* **1998**, *10*, 467–470.
- (3) Burkett, S. L.; Sims, S. D.; Mann, S. *Chem. Commun.* **1996**, 1367–1368.
- (4) Mercier, L.; Pinnavaia, T. J. *Adv. Mater.* **1997**, *9*, 500–503.
- (5) Mezziani, M. J.; Zajac, J.; Jones, D. J.; Roziere, J.; Partyka, S. *Langmuir* **1997**, *13*, 5409–5417.
- (6) Diaz, J. F.; Balkus, K. J.; Bedioui, F.; Kurshev, V.; Kevan, L. *Chem. Mater.* **1997**, *9*, 61–67.
- (7) Rao, S. Y. V.; De Vos, D. E.; Jacobs, P. A. *Angew. Chem., Int. Ed. Engl.* **1997**, *36*, 2661–2663.
- (8) Kresge, C. T.; Leonowicz, M. E.; Roth, W. J.; Vartulli, J. C.; Beck, J. S. *Nature* **1992**, *359*, 710–712.
- (9) Beck, J. S.; Vartulli, J. C.; Roth, W. J.; Leonowicz, M. E.; Kresge, C. T.; Schmitt, K. D.; Chu, C. T.-W.; Olson, D. H.; Sheppard, E. W.; McCullen, S. B.; Higgins, J. B.; Schlenker, J. L. *J. Am. Chem. Soc.* **1992**, *114*, 10834–10843.

- (10) Sutra, P.; Brunel, D. *Chem. Commun.* **1996**, 2485–2486.
- (11) Moller, K.; Bein, T. *Chem. Mater.* **1998**, *10*, 2950–2963.
- (12) Feng, X.; Fryxell, G. E.; Wang, L. Q.; Kim, A. Y.; Liu, J.; Kemner, K. M. *Science* **1997**, *276*, 923–926.
- (13) Shepard, D. S.; Zhou, W.; Maschmeyer, T.; Matters, J. M.; Roper, C. L.; Parsons, S.; Johnson, B. F. G.; Duer, M. J. *Angew. Chem., Int. Ed. Engl.* **1998**, *37*, 2719–2723.
- (14) Moller, K.; Bein, T.; Fischer, R. X. *Chem. Mater.* **1999**, *11*, 665–673.
- (15) Sims, S. D.; Burkett, S. L.; Mann, S. *Mater. Res. Soc. Symp. Proc.* **1996**, *431*, 77–82.
- (16) Macquarrie, D. J. *Chem. Commun.* **1996**, 1961–1962.
- (17) Fowler, C. E.; Burkett, S. L.; Mann, S. *Chem. Commun.* **1997**, 1769–1770.
- (18) Bانونneau, F.; Leite, L.; Fontlupt, S. *J. Mater. Chem.* **1999**, *9*, 175–178.
- (19) Van Rhijn, W. M.; Devos, D. E.; Sels, B. F.; Bossaert, W. D.; Jacobs, P. A. *Chem. Commun.* **1998**, 317–318.
- (20) Van Rhijn, W.; De Vos, D.; Bossaert, W.; Bullen, J.; Wouters, B.; Grobet, P.; Jacobs, P. *Stud. Surf. Sci. Catal.* **1998**, *117*, 183–190.
- (21) Huo, Q. S.; Margolese, D. I.; Stucky, G. D. *Chem. Mater.* **1996**, *8*, 1147–1160.

groups and by their accessibility. The grafting rates depend on the reactivity of precursors, diffusion limitations, and steric factors.

An alternative approach to modify the internal surfaces of MCM-41 is by direct synthesis, which is based on the co-condensation of siloxane and organosiloxane precursors in a templating environment. Siloxane precursors function as building blocks to construct the framework while the organosiloxanes contribute both framework silicate units and the organic surface functional groups. This single-step synthesis can produce mesoporous solids with high loadings of organic functional groups and homogeneous surface coverage within a relatively short preparation time.² However, one must be cautious in choosing precursors since the reaction involves basic conditions during the hydrothermal synthesis and acidic conditions during surfactant removal. Thus, the Si-C bond in a precursor should be hydrolytically stable under these circumstances.^{22,23}

The present study reports structural, chemical, and physical properties of vinyl-modified MCM-41 samples prepared by using both PSG and direct synthesis. The major features of this study are comparisons of products from both methods with respect to efficiencies of the synthetic routes, precursor effects, vinyl group concentrations, the locations of vinyl groups in the mesoporous products, the hydrothermal stability of vinyl-functionalized samples, and qualitative observations of solvent absorption properties.

Experimental Section

Materials. Distilled deionized water (DDI) and analytical grade chemicals from the following suppliers were used as purchased for all sample preparations: tetraethoxysilane (TEOS, 96%) (TCI), tetramethoxysilane (TMOS, 98%), vinyltrichlorosilane (VTCS), cetyltrimethylammonium bromide (CTAB), NaOH (97%), bromine, mesitylene (98%), hexanes (98.5%), and dichloromethane (99.6%) (all Aldrich); vinyltriethoxysilane (VTES), vinyltrimethoxysilane (VTMS) (both UCT).

Instrumentation. Powder X-ray diffraction (PXRD) data were collected at room temperature using either the Siemens D-500 or D-5005 wide-angle diffractometers with Cu K α radiation. X-ray photoelectron spectroscopy (XPS) was performed at the University of Minnesota Surface Analysis Center, using a Physical Electronics PHI5400 XPS instrument with a Mg anode (1253.6 eV) operating at 300 W. Charging effects were corrected by adjusting the C 1s peak to 284.6 eV. Spectra of Si 2p, O 1s, Br 3d, and C 1s were recorded. Sensitivity factors supplied with the instrument were employed to calculate atomic ratios. N₂ adsorption measurements were performed with a Micromeritics ASAP 2000 V3.00 sorption analyzer. Surface areas were calculated by the Brunauer-Emmett-Teller (BET) method and pore sizes by the Barrett-Joyner-Halenda (BJH)²⁴ and Horvath-Kawazoe (HK) methods.²⁵ All samples were dried at 100 °C for a minimum of 5 h under vacuum (2 μ mHg) before carrying out nitrogen adsorption experiments. Both ¹³C and ²⁹Si MAS solid-state NMR experiments were performed on a 400 MHz Chemagnetics solid-state NMR spectrometer. ¹³C MAS NMR spectra were obtained at 100.63 MHz with 7 kHz applying 90°

pulses and 2.0 s pulse delays. To enhance carbon sensitivity, cross-polarization (CP) techniques were employed. ²⁹Si MAS NMR spectra were recorded at 79.49 MHz applying 90° pulses, 300 s pulse delays, and 5.0 ms contact time, with samples in 5.0 mm zirconia rotors spinning at 7 kHz. UV-vis spectra were recorded on a Hewlett-Packard 8254A diode array spectrometer. Thermogravimetric analysis (TGA) was carried out on a Perkin-Elmer TGA-7 thermal analyzer connected to a PC via a TAC7/DX thermal controller. The samples were heated from 50 to 800 °C at 10 °C/min under nitrogen. Chemical analyses for C, H, N, and Br were carried out by Atlantic Microlab Inc.

Small-angle neutron scattering (SANS) experiments were performed at the SAND beamline of the Intense Pulsed Neutron Source (IPNS) at Argonne National Laboratory, Argonne, IL. Samples were loaded into a Suprasil cylindrical cell with a 1 mm path length. The scattered neutrons were measured using a 128 \times 128 array of position-sensitive, gas-filled, 40 \times 40 cm², proportional counters with the wavelengths measured by time-of-flight. Data in the Q range of 0.0035–0.8 Å⁻¹ were taken in a single measurement.

Preparation of Purely Siliceous MCM-41. CTAB (4.38 g) was dissolved in 200 g of DDI water containing 1.10 g of NaOH. While the surfactant solution was stirred vigorously, 15.22 g of TMOS was added quickly. The mixture turned white within 5 s and was stirred for 24 h at room temperature, followed by heating at 90 °C for an additional 24 h without stirring. The product was isolated by vacuum filtration on a Büchner funnel and washed alternately with DDI water and methanol until the pH of the washings was neutral. The resulting powder was dried in air at ambient temperature. The surfactant was removed by acid/solvent extraction, using a solution of 500 mL of methanol and 7.0 g of aqueous HCl (37%) per 4–6 g of sample. This mixture was refluxed for 1 day, then filtered, and washed with methanol until the pH was neutral. The isolated product was vacuum-dried at 90 °C for 1 day.

Grafting Vinyl Groups onto MCM-41 Using VTCS as a Vinyl Precursor (v-gr-MCM-41). Siliceous MCM-41 (0.8 g) contained in a 100 mL round-bottom flask was dried at 100 °C in a vacuum oven for 24 h. The hot flask containing the sample was sealed with a septum immediately before removal from the vacuum oven to keep out moisture from the air. Dry toluene (40 mL) was injected into the flask. While the solution was stirred gently, 1.0 mL of VTCS (1.3 g, 7.9 mmol) was injected. The resulting mixture was stirred for 10 min at room temperature and then refluxed for 24 h in an oil bath. A drying tube was attached to the reflux apparatus to minimize the influence of moisture. The product was vacuum filtered and washed with dry toluene. To remove ungrafted VTCS, the sample was dried at 100 °C for 24 h in a vacuum oven. Last, the sample was washed with DDI water to hydrolyze remaining chloride groups and then dried again at 100 °C for 24 h in a vacuum oven.

One-Pot Syntheses of v-MCM-41(L) and v-MCM-41(H). v-MCM-41(L) was prepared according to our previously reported procedures.¹ The molar composition of reagents was 1 TEOS:0.25 VTES:0.15 CTAB:0.38 NaOH:125 H₂O. v-MCM-41 containing a higher concentration of vinyl groups was prepared by using methoxy-based precursors. The molar ratio of reagents was 1 TMOS:0.47 VTMS:0.18 CTAB:0.37 NaOH:147 H₂O. CTAB (2.19 g) was dissolved in 90 g of DDI water containing 0.50 g of NaOH. A mixture of 2.37 g of VTMS and 5.18 g of TMOS was poured to the surfactant solution while stirring vigorously. Condensation occurred within 5 s. The resulting white product was stirred at room temperature for 1 h and then heated at 90 °C for 24 h under static conditions. The product isolation and surfactant removal were carried out by the same method described above.

Preparation of Large-Pore v-MCM-41 (LP-v-MCM-41) from a Direct Synthesis. A similar v-MCM-41 with larger pores was synthesized by adding auxiliary swelling agents to the stirred reaction mixture. A mixture of VTES (1.93 g) and TEOS (8.33 g) was added quickly to a surfactant solution (2.19 of CTAB in 100 g of DDI water) containing NaOH (0.6 g). After 5 min, a solution of mesitylene (4.32 g) and hexanes (1.55 g) was added to the stirred mixture. The resulting thick mixture

(22) Sommer, L. H.; Goldberg, G. M.; Dorfman, E.; Whitmore, F. C. *J. Am. Chem. Soc.* **1946**, *68*, 1083.

(23) Sommer, L. H.; Baughman, G. A. *J. Am. Chem. Soc.* **1961**, *83*, 3346.

(24) Barrett, E.; Joyner, L. G.; Halenda, P. P. *J. Am. Chem. Soc.* **1951**, *73*, 373–380.

(25) Horvath, G.; Kawazoe, K. *J. Chem. Eng. Jpn.* **1983**, *16*, 470–475.

was stirred and shaken vigorously for 10 min and then heated at 85 °C for 2 days with stirring. The molar composition of this mixture was 1 TEOS:0.25 VTES:0.15 CTAB:0.38 NaOH:139 H₂O:0.9 mesitylene:0.45 hexanes.

Bromination of v-MCM-41. The v-MCM-41 samples were brominated either in the gas phase or in solution. For gas-phase bromination, about 2–3 mL of liquid bromine was placed in a 100 mL round-bottom flask with a sidearm, and the v-MCM-41 sample was placed in a 100 mL Erlenmeyer flask. The two flasks were interconnected by combination of distilling and vacuum distilling adapters. The bromine vapor was transferred to the flask containing 0.35–0.45 g of v-MCM-41 with nitrogen gas as a carrier for 10 min. During the bromine vapor transportation, the v-MCM-41 powder was agitated for better mixing. After v-MCM-41 was exposed to bromine vapor, the color of the sample changed to orange. The bright orange materials were stored in a closed flask for 50 min and exposed to the air to remove adsorbed excess bromine. To remove excess bromine more effectively, it was necessary to use a vacuum. The resulting product was white. In solution phase bromination, CH₂Cl₂ was used as a solvent. v-MCM-41L (0.50 g) was dispersed in CH₂Cl₂, and then ca. 0.12 g of Br₂ was added. The mixtures were stirred for 2 or 6 days. The brominated samples were isolated by vacuum filtration, rinsed with CH₂Cl₂, and dried at 100 °C for 24 h. The brominated products were white.

Kinetic Study of the Bromination Reaction. The bromination reaction was monitored by UV–vis spectroscopy, following the decay of the UV absorption at $\lambda_{\text{max}} = 412$ nm. An initial bromine stock solution was prepared by adding ~1 drop of bromine to 20 mL of CH₂Cl₂ or CCl₄. For each experiment, the concentration of the bromine stock solution was adjusted to give an initial UV absorbance value of approximately one at $\lambda = 412$ nm in a 1 cm quartz cuvette. Approximately 1 mg of vinyl-modified MCM-41 was added to the cuvette and stirred. After given lengths of time, stirring was stopped, the cuvette was centrifuged for 3 min to separate all of the powder from the supernatant, and UV–vis spectra of the supernatant bromine solution were obtained. A control experiment was carried out in a similar way using a sample of purely siliceous MCM-41.

Results and Discussion

Nomenclature and General Synthesis Considerations. The grafted product was denoted v-gr-MCM-41. To maximize the number of available surface silanol groups in purely siliceous MCM-41, the surfactant was removed from the support by extraction with HCl/methanol;¹ the alternate surfactant removal method, calcination, leads to condensation of silanol groups, resulting in fewer anchoring sites.

Vinyl groups were also directly incorporated in the mesoporous phase by co-condensation of either 1 VTES:4 TEOS or 1 VTMS:2.1 VTMS (molar ratios) in a surfactant environment. To distinguish products from these reactions from the vinyl-grafted MCM-41 sample, vinyl-functionalized MCM-41 from direct syntheses were labeled v-MCM-41L¹ and v-MCM-41H, where L and H indicate low and high concentrations of vinyl groups, respectively. These compositions were chosen for our study, as they represented the maximum vinyl loadings obtainable by our method that still resulted in hexagonally ordered structures for each set of precursors. With ethoxy precursors, hexagonally ordered v-MCM-41 structures were obtained up to VTES/TEOS ratios of 0.25. At higher ratios the product structures were disordered. By utilizing methoxy-based precursors (VTMS and TMOS), which hydrolyze faster than their ethoxy analogues, well-ordered v-MCM-41 could be synthesized

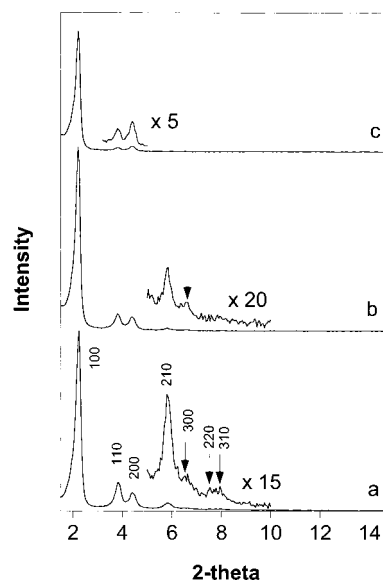


Figure 1. Powder XRD patterns of (a) siliceous MCM-41 after surfactant extraction, (b) vinyl-MCM-41 grafted with VTCS for 1 day (v-gr-MCM-41), and (c) sample (b) after gas-phase bromination.

with higher loadings of vinyl groups. We had observed previously in the direct synthesis of thiol-MCM-41 that fast hydrolysis was critical to permit the formation of ordered MCM-41 with high loadings of organic groups.²

In the preparation of large-pore v-MCM-41 (LP-v-MCM-41) using the direct synthesis method, the order of adding swelling agents and the nature of siloxane precursors had a significant influence on the pore diameters. When swelling agents (a mixture of mesitylene and hexanes) were added to the template solution before addition of siloxane precursors, the pore size of v-MCM-41 did not increase. However, an increase in the pore size of v-MCM-41 was attained by adding the swelling agents to the reaction bottle in which VTES and TEOS were already partially polymerized in the template solution. Since VTES and TEOS hydrolyzed and condensed in a period of ~20 min under our conditions, the initial mesostructure was only weakly polymerized when mesitylene and hexanes were added after 5 min. The loosely condensed framework could be easily expanded by swelling agents within the micellar arrays. Pore sizes of v-MCM-41 samples could not be increased when precursors with methoxy groups were employed. Because of the fast hydrolysis and condensation of these precursors in the template solution, the framework became rigid quickly, which may have prevented expansion of the pore size.

Structures of Vinyl-Modified MCM-41 Samples and Their Derivatives. Figure 1 shows PXRD patterns of MCM-41 and samples derived by grafting with VTCS. The PXRD pattern of siliceous MCM-41 shows seven low-angle reflections and a d_{100} spacing value of 4.0 nm. Upon grafting vinyl groups to the surface using VTCS (v-gr-MCM-41), the d_{220} and d_{310} reflections were no longer observed, and the overall intensity decreased slightly. Bromination led to a further decrease in intensity, as well as loss of two more reflections (d_{210} , d_{300}). After each treatment, the peak positions remained virtually constant, suggesting that the structural ordering of the MCM-41 channels remained.

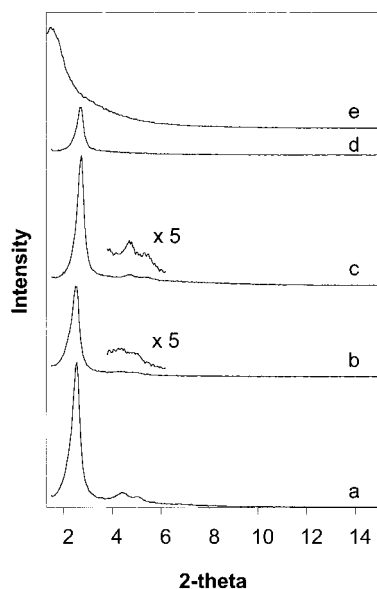


Figure 2. Powder XRD patterns of (a) v-MCM-41L (1 VTES:4 TEOS) after surfactant extraction, (b) sample (a) after gas-phase bromination, (c) v-MCM-41H (1 VTMS:2.1 TMOS) after surfactant extraction, (d) sample (c) after gas-phase bromination, and (e) LP-v-MCM-41 (1 VTES:4 TEOS) after surfactant extraction.

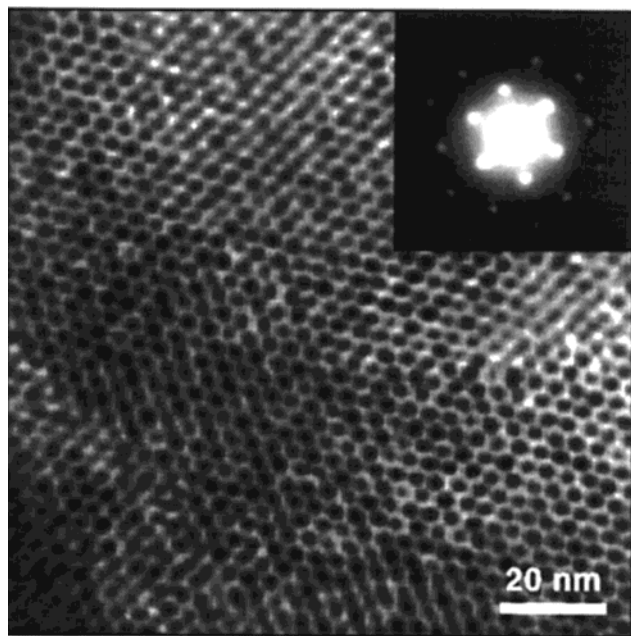


Figure 3. TEM image of a region of v-MCM-41 after surfactant extraction. The inset shows the selected area electron diffraction pattern from this region.

Figure 2 presents the PXRD patterns of products from the direct co-condensation reaction, v-MCM-41(L and H), the corresponding brominated samples, and LP-v-MCM-41. Except for LP-v-MCM-41, which exhibited a single broad reflection, the surfactant-extracted v-MCM-41 samples displayed three distinct reflections (d_{100} , d_{110} , d_{200}), which provide evidence for a hexagonal arrangement. The transmission electron microscopy (TEM) image and electron diffraction pattern (Figure 3) confirm the hexagonal symmetry of v-MCM-41L.¹ The relative intensities of higher angle peaks with respect to d_{100} decreased as the concentration of vinyl groups increased and decreased further upon bromination.

While the intensity reduction may be partially attributed to lower local order, such as variations in the wall thickness, we believe that it is mostly due to contrast matching between the amorphous silicate framework and organic moieties that are located inside the channels of MCM-41. Marler et al.²⁶ observed that the PXRD peak intensities of boron-containing MCM-41 (B-MCM-41) were related to the density of organic sorbates incorporated in B-MCM-41. When organic sorbates having higher density were loaded in B-MCM-41, all PXRD intensities systematically decreased due to the smaller difference of scattering contrast between organic sorbates and silicate walls of B-MCM-41. Since the organic sorbates were liquid, they were assumed to be homogeneously distributed inside B-MCM-41. Analogously, the systematic decreases of the PXRD peak intensities in the brominated v-MCM-41 samples resulted from the reduction in scattering contrast between the channel walls and organic groups after bromine was added, implying that vinyl groups were uniformly distributed throughout the channel surfaces. For the grafted sample, v-gr-MCM-41, the intensity of the d_{110} reflection decreased to a greater extent after bromination than the other reflections (see Figure 1c), suggesting a different, possibly more localized distribution of organic groups in the sample (see below).

The d_{100} spacings and pore volumes decreased from MCM-41 to v-MCM-41L to v-MCM-41H, as the vinyl-siloxane content of the reaction mixture increased (see Table 1). Similar behavior was observed by Burkett et al. in the direct synthesis of phenyl-modified mesoporous sieves^{3,17} and by Lim et al. for directly synthesized thiol-MCM.²⁷ This trend can be rationalized in terms of different interactions between the cationic surfactant molecules and the silicate or organosilicate precursors during the hydrothermal reaction. When the MCM-41 phase is formed via surfactant-silicate self-assembly under basic conditions, the negatively charged silicate species interact electrostatically with positively charged surfactant headgroups. The surfactant-silicate interface, in which vinyl groups may be located, becomes an electrostatically neutral region due to the charge compensation. At increasing vinyl concentrations the density of silanol groups in this interface region decreases, and fewer surfactant molecules are required for charge balance. This leads to contraction of the cylindrical micelle size in v-MCM-41 with higher concentrations of organic surface groups. An alternate explanation would invoke stronger hydrophobic interactions between the vinyl groups and the surfactant tails; as a result, the vinyl groups may be drawn further into the surfactant micelles, leading to the smaller channel diameters that were observed.

Solid State ^{13}C and ^{29}Si MAS NMR. Organic functional groups were identified by solid state ^{13}C CP MAS NMR. The solid state ^{13}C CP MAS NMR spectra displayed three resonances for all vinyl-modified MCM-41 samples, corresponding to vinyl carbons at 129 and 135 ppm and methanol (solvent) at 50 ppm vs TMS (Figure 4a). These data confirmed that vinyl groups were not damaged by either PSG or direct syntheses,

(26) Marler, B.; Oberhagemann, U.; Vortmann, S.; Gies, H. *Microporous Mater.* **1996**, *6*, 375–383.

(27) Lim, M. H.; Stein, A., unpublished results.

Table 1. XRD d_{100} Spacing and Nitrogen Adsorption Data of Siliceous MCM-41 and Organically Modified MCM-41 Samples

sample	XRD d_{100} spacing (nm)	BET surf. area (m ² /g)	pore vol (cm ³ /g)	wt-corrected surf. area reduction ^a (%)	wt-corrected pore vol reduction ^a (%)	bromine content
siliceous MCM-41	4.0	1050	0.93			
v-gr-MCM-41	4.0	998	0.68			
brominated v-gr-MCM-41	4.0	756	0.46	1	12	23.4
v-MCM-41L	3.5	1424	0.82			
brominated v-MCM-41L	3.5	932	0.57	15	10	22.7
v-MCM-41H	3.3	1082	0.71			
brominated v-MCM-41H	3.3	563	0.36	20	22	35.5
LP-v-MCM-41	5.7	986	1.19			

^a Weight corrections were performed based on the elemental analysis data of brominated samples. For example, the weight-corrected surface area of v-gr-MCM-41 was calculated by applying a weight correction factor (0.766) that was determined by subtracting the fraction of bromine (0.234) from the unit mass. Thus, the resulting weight-corrected surface area of v-gr-MCM-41 was 985 m²/g (756 m²/g/0.7658).

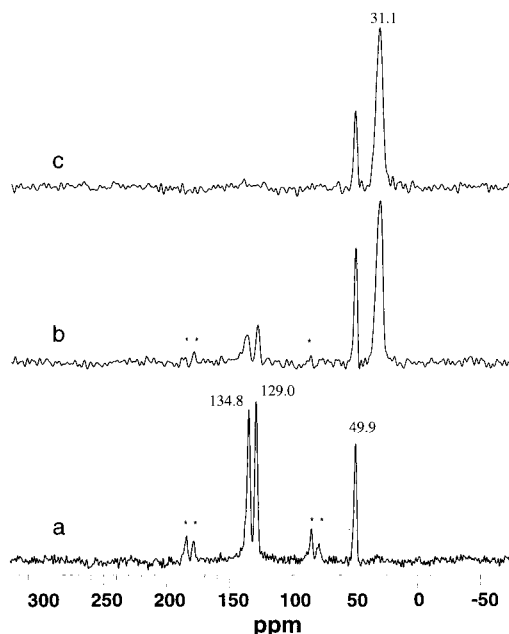


Figure 4. ¹³C CP MAS NMR spectra of (a) v-MCM-41L, (b) v-MCM-41L brominated for 2 days, and (c) v-MCM-41L brominated for 6 days. The asterisks indicate spinning sidebands.

and all surfactant molecules were completely removed by HCl/methanol extraction.

Solid state ²⁹Si MAS NMR provides information about the silicon environment and about the degree of organic functionalization. To permit quantitation of the peak areas, ²⁹Si MAS NMR spectra were obtained using a single pulse experiment. Table 2 summarizes observed resonances from ²⁹Si MAS NMR spectra and the corresponding relative peak areas. The ²⁹Si MAS NMR spectra of siliceous MCM-41 and vinyl-grafted MCM-41 samples are presented in Figure 5. Siliceous MCM-41 exhibited two resonances at −102.5 and −112.4 ppm, corresponding to HOSi(OSi)₃ (Q³) and Si(OSi)₄ (Q⁴) silicate species, respectively. The ratio of the relative peak areas of the deconvoluted peaks, Q⁴/Q³, was 1.8. This ratio was comparable with other calcined MCM-41 samples.²⁸ Upon grafting the surface with vinyl groups using VTCS, the ²⁹Si MAS NMR spectrum showed two additional resonances at −61.3 and −70.3 ppm that were assigned to R–Si(OH)₂(OSi) (T¹) and

R–Si(OH)(OSi)₂ (T²) centers, respectively. As expected, the grafting process also resulted in a decrease in the intensity of the Q³ resonance and a concomitant increase in the intensity of the Q⁴ resonance.

Figure 6 displays ²⁹Si MAS NMR spectra of v-MCM-41L and v-MCM-41H, which were prepared by the direct synthesis. Unlike vinyl-grafted MCM-41 samples, v-MCM-41(L and H) showed only T³ (−80 ppm) and T² (−71 ppm) resonances, which suggests that vinyl groups were more tightly incorporated in the wall surfaces. In the case of v-MCM-41H, the ratio of surface hydroxyls to organic functional groups (Q³/T) was 0.9 for v-MCM-41H and 2.8 for v-MCM-41L. No resonances corresponding to Si attached to unreacted methoxy groups were observed.²⁹

Nitrogen Adsorption Measurements. The N₂ adsorption–desorption isotherms for siliceous MCM-41, v-gr-MCM-41, and the corresponding brominated samples are displayed in Figure 7. All samples showed type IV isotherms,³⁰ characteristic of mesoporous materials according to the IUPAC classification.³¹ The isotherms of siliceous MCM-41 and the brominated v-gr-MCM-41 sample exhibited virtually no hysteresis loops at relative pressures (p/p_0) below 0.4. This phenomenon may result from the instability of the liquid nitrogen meniscus inside the narrow channels.^{32,33} In contrast, v-gr-MCM-41 exhibited a large hysteresis loop in the p/p_0 region between 0.2 and 0.36. While the hysteresis may be associated with capillary condensation in ink-bottle pores, other effects such as network effects, the nature of the framework, the adsorbate, and the temperature can influence the shape of the isotherm, so that interpretation is difficult for this hybrid material.³⁴

Figure 8 shows the N₂ adsorption–desorption isotherms for the vinyl-modified MCM-41 samples prepared from the direct syntheses and the corresponding samples after bromination. A reversible type IV isotherm was observed only for the v-MCM-41L sample. All other samples showed slight hysteresis loops. In the case of brominated v-MCM-41H, the condensation step was not well developed. The specific surface areas of all

(29) Brinker, C. J.; Scherrer, G. *Sol–Gel Science: the Physics and Chemistry of Sol–Gel Processing*; Academic: San Diego, 1989.

(30) Gregg, S. J.; Sing, K. S. W. *Adsorption, Surface Area and Porosity*, 2nd ed.; Academic Press Inc.: San Diego, 1982.

(31) Everett, D. H. *Pure Appl. Chem.* **1972**, *31*, 578.

(32) Branton, P. J.; Hall, P. G.; Sing, K. S. W. *J. Chem. Soc., Chem. Commun.* **1993**, 1257–1258.

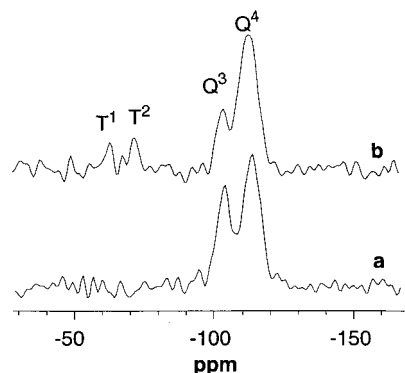
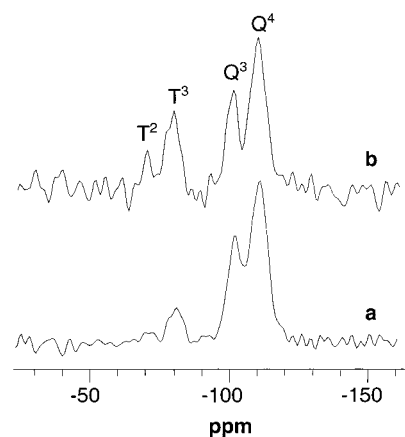
(33) Branton, P. J.; Hall, P. G.; Sing, K. S. W.; Reichert, H.; Schüth, F.; Unger, K. K. *J. Chem. Soc., Faraday Trans.* **1994**, *90*, 2965–2967.

(34) Sing, K. S. W. *Adv. Colloid Interface Sci.* **1998**, *77*, 3–11.

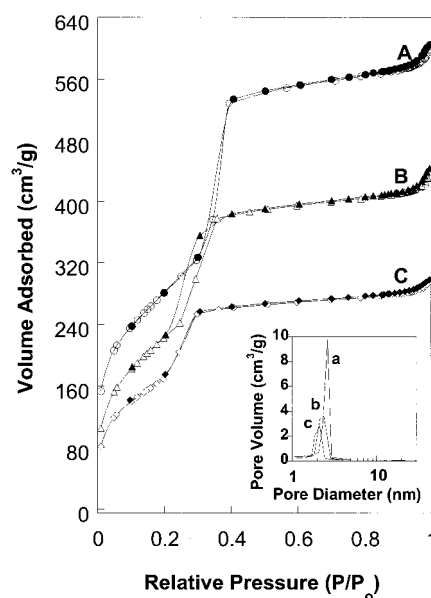
(28) Voegtlin, A. C.; Matijasic, A.; Patarin, J.; Sauerland, C.; Grillet, Y.; Huve, L. *Microporous Mater.* **1997**, *10*, 137–147.

Table 2. ^{29}Si MAS NMR Data for Surfactant-Free Siliceous MCM-41 and Vinyl-Functionalized MCM-41 Samples: Chemical Shifts, Corresponding Relative Peak Areas Obtained by Curve Deconvolution, and Relative Peak Area Ratios

sample	δ (ppm)/relative peak area ^a							
	T ¹	T ²	T ³	Q ²	Q ³	Q ⁴	Q/T	Q ⁴ /(Q ³ + T ⁿ)
MCM-41					-102.5 36%	-112.4 64%		1.8
v-gr-MCM-41	-61.3 4%	-70.3 8%			-101.4 16%	-110.8 72%	7.7	4.4
v-MCM-41L		-70.5 2%	-80.1 9%		-101.6 31%	-110.6 58%	8.3	1.9
v-MCM-41 H		-71.4 5%	-80.4 21%		-101.9 23%	-111.2 50%	2.8	1.0

^a Relative peak areas are shown in boldface.**Figure 5.** ^{29}Si MAS NMR spectra of (a) siliceous MCM-41 after surfactant-extraction and (b) vinyl-MCM-41 grafted with VTCS for 1 day (v-gr-MCM-41).**Figure 6.** ^{29}Si MAS NMR spectra of (a) surfactant-extracted v-MCM-41L (1 VTMS:4 TMOS) and (b) surfactant-extracted v-MCM-41H (1 VTMS:2.1 TMOS).

samples were calculated by the BET method. The pore sizes were obtained from the BJH²⁴ and HK²⁵ models (Table 3). The BET surface area (SA) of siliceous MCM-41 was 1050 m²/g, and the pore volume (PV) was 0.93 cm³/g, typical values for MCM-41 samples prepared under basic conditions. The sample exhibited a narrow pore size distribution. The PV and pore diameters decreased in the course of functionalization (vinylsilation and bromination). Similarly, the v-MCM-41L and H samples from direct synthesis showed reductions of SA, PV, and pore diameters upon bromination. Estimates of pore diameters are quite important in these types of materials because the pore sizes determine accessibility of reagents and other guest molecules. We have employed both the BJH and HK models to estimate wall thickness. The BJH model always provided smaller pore diameters than the HK model. These

**Figure 7.** Nitrogen adsorption-desorption isotherms of (A) siliceous MCM-41, (B) v-gr-MCM-41, and (C) brominated v-gr-MCM-41. The inset shows the pore size distribution of (a) siliceous MCM-41, (b) v-gr-MCM-41, and (c) brominated v-gr-MCM-41.

results are in agreement with several previous studies, which have reported the underestimation of pore diameters by the BJH calculation.³⁵⁻³⁷

Table 1 summarizes the d_{100} spacings, the surface areas, and pore volumes of the vinyl-functionalized MCM-41 samples and the corresponding brominated samples. After vinyl groups were anchored on siliceous MCM-41, the specific pore volume decreased by 27% whereas the decline of the specific surface area was only 5%, based on the direct comparison of nitrogen adsorption data. However, since both specific surface area and pore volume are associated with mass, mass changes should be considered in these comparisons. Changes in surface area and pore volume after bromination were therefore corrected by taking into account the organic contributions based on the elemental analysis of the corresponding brominated samples. Brominated v-gr-MCM-41 exhibited a 1% decrease of surface area and a 12% reduction of pore volume. In contrast, the v-MCM-41L and v-MCM-41H samples from the direct synthesis

(35) Ravikovitch, P. I.; Odomehnaill, S. C.; Neimark, A. V.; Schüth, F.; Unger, K. K. *Langmuir* **1995**, *11*, 4765-4772.(36) Kruk, M.; Jaroniec, M.; Sayari, A. *J. Phys. Chem. B* **1997**, *101*, 583-589.(37) Ravikovitch, P. I.; Wei, D.; Chueh, W. T.; Haller, G. L.; Neimark, A. V. *J. Phys. Chem. B* **1997**, *101*, 3671-3679.

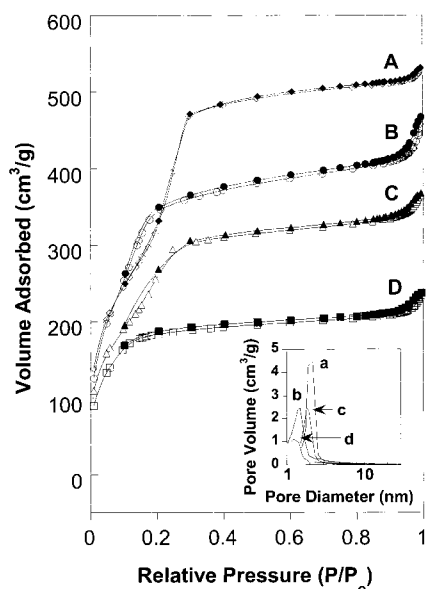


Figure 8. Nitrogen adsorption–desorption isotherms of (A) v-MCM-41L, (B) v-MCM-41H, (C) brominated v-MCM-41L, and (D) brominated v-MCM-41H. The inset shows the BJH pore size distributions of (a) v-MCM-41L, (b) v-MCM-41H, (c) brominated v-MCM-41L, and (d) brominated v-MCM-41H.

showed 15 and 20% decreases in surface area and 10 and 22% reductions in pore volume after bromination, respectively. These results are quite striking because the surface area of the grafted sample was not affected by bromination. The negligible decrease of the surface area of v-gr-MCM-41 can be rationalized as a geometric effect. Since both surface area and pore volume are calculated from nitrogen adsorption experiments, the accessibility of nitrogen molecules to surface features influences these values. When vinylsilane is anchored onto the surface of MCM-41, grafted vinylsilanes also contribute to increase the surface area. Because the regions between vinyl groups and the surface are spacious enough to accommodate nitrogen molecules (based on a MM2 calculation with the CS Chem 3D program suite),³⁸ the surface area reduction due to the grafting process is compensated by the surface area generated from the vinylsilane groups. In v-MCM-41(L and H), vinyl groups are tightly bound to the MCM-41 surfaces; bromination of the vinyl groups fills the space between the organic groups and the silica surface, making it less accessible to nitrogen molecules. Thus, the surface area available to nitrogen decreases. On the other hand, weight-corrected pore volumes of *all* vinyl-functionalized MCM-41 samples decreased after bromination. This provides strong evidence that vinyl groups are located inside the channel surfaces.

LP-v-MCM-41 exhibited a type IV isotherm displaying large hysteresis (see Figure 9). Its BET surface area and pore volume were 986 m²/g and 1.19 cm³/g, respectively. Compared to v-MCM-41L, the pore size of LP-v-MCM-41 increased from 2.2 to 3.8 nm on the basis of the BJH method, but its pore size distribution became wider than that of v-MCM-41L.

SANS Experiments. Neutron scattering density contrast matching experiments were performed using

small-angle neutron scattering. The intensity distribution $I(q)$ for small-angle scattering can be analyzed by using the Guinier approximation, which is described by

$$I(q) = NV^2(\Delta\rho)^2 \exp(-q^2 R_g^2/3)$$

where N is the number of particles, V the particle volume, $(\Delta\rho)$ the difference in the scattering length density of the particle and any solvent present, R_g the radius of gyration, and q the wave vector (which is related to the d spacing via $q = 2\pi/d$).³⁹ The variation of intensity with scattering angle in the small-angle scattering region (Guinier region) can be described by various power laws with exponents that are characteristic for a given geometry. Figure 10 shows a $\log(I)$ vs $\log(q)$ SANS plot for v-MCM-41L and for a siliceous MCM-41 sample prepared in the same way without any vinyltriethoxysilane. Both samples were saturated with a 66% D₂O/34% H₂O solution. Because the neutron scattering density for this solution matched that of silica, the silica signal was practically nullified in the SANS pattern of the pure silica MCM-41.^{40–42} In the case of v-MCM-41L, significant signal intensity remained in the $q < 0.08 \text{ \AA}^{-1}$ region (power law slope of linear region: -3.5), confirming that vinyl groups were present in the mesopore channels, not in a completely separate phase. This result was consistent with the decreases in pore volumes and pore diameters that had been observed by nitrogen adsorption measurements of brominated v-MCM-41L samples. The concentration of the surface groups was too low to result in a d_{100} scattering peak by the SANS technique.

Kinetic Study of the Bromination of Vinyl-Functionalized MCM-41 Samples. In a preliminary study of the bromination of v-MCM-41L in dichloromethane, a remarkably slow reaction rate was observed at room temperature; complete bromination required several days.¹ The slow bromination was confirmed by solid state ¹³C CP MAS NMR spectra of v-MCM-41L reacted with bromine for 2 or 6 days (see Figure 4). After bromination, a broad peak at 31.1 ppm confirmed the presence of C–Br bonds. Resonances due to vinyl carbon atoms were still present after a 2 day bromination but disappeared completely after a 6 day reaction, indicating that all vinyl groups were accessible to bromine. This reaction was unusually slow compared to solution bromination of unsaturated organic compounds even with bulky protecting groups.⁴³ In addition, the rate was slower than expected for unhindered diffusion of Br₂ (kinetic diameter: 0.35 nm) through 2.2 nm diameter mesopore channels.⁴⁴

For quantitative measurements, the bromination reaction was monitored by UV–vis spectroscopy. Figure 11 compares the intensity decreases of the bromine

(39) Carrado, K. A.; Thiyagarajan, P.; Winans, R. E.; Botto, R. E. *Inorg. Chem.* **1991**, *30*, 794–799.

(40) Bradley, K. F.; Chen, S. H.; Thiyagarajan, P. *Phys. Rev. A* **1990**, *42*, 6015–6023.

(41) Glinka, C. J.; Nicol, J. M.; Stucky, G. D.; Ramli, E.; Margolese, D.; Huo, Q.; Higgins, J. B.; Leonowicz, M. E. *J. Porous Mater.* **1996**, *3*, 93–98.

(42) Bendedouch, D.; Chen, S. H.; Koehler, W. C. *J. Phys. Chem.* **1983**, *87*, 153–159.

(43) Brown, R. S.; Slebocka-Tilk, H.; Bennet, A. J.; Bellucci, G.; Bianchini, R.; Ambrosetti, R. *J. Am. Chem. Soc.* **1990**, *112*, 6310–6316.

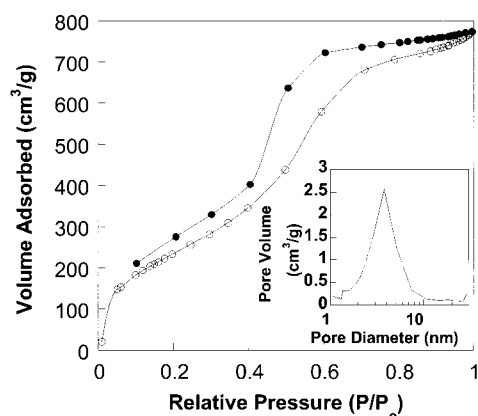
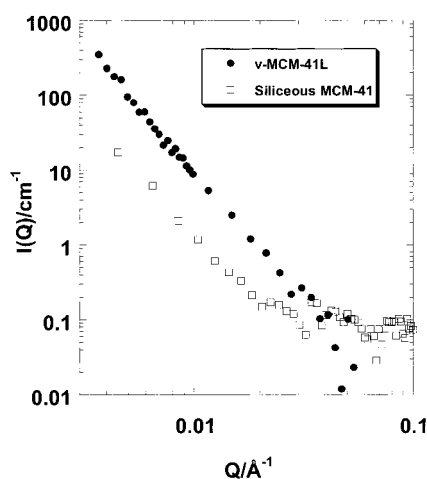
(44) Gupta, V.; Nivarthi, S. S.; McCormick, A. V.; Davis, H. T. *Chem. Phys. Lett.* **1995**, *247*, 596–600.

(38) *CS Chem 3D Pro*; 3.5.1 ed.; Cambridge Soft Corporation: Cambridge, 1997.

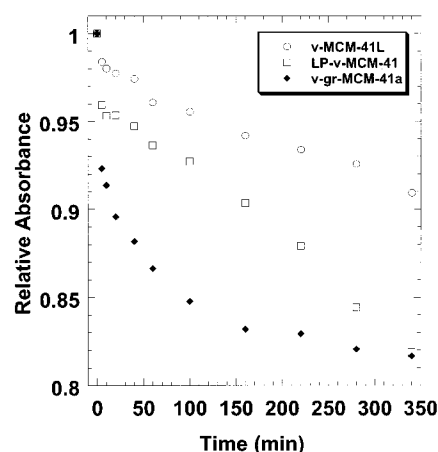
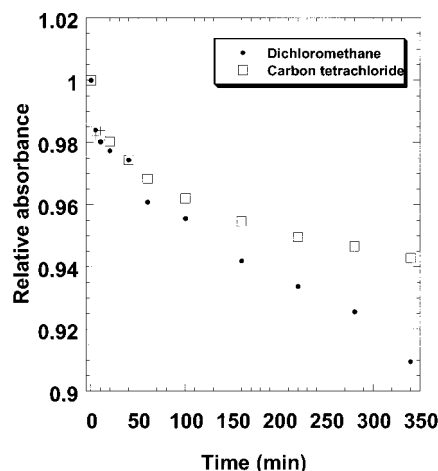
Table 3. Calculated Pore Diameters and Wall Thicknesses of Siliceous MCM-41 and Organically Modified MCM-41 Samples, Using BJH and HK Models

sample	d_{100} (nm)	a_0^a (nm)	pore diameter (nm)		wall thickness (nm)	
			BJH	HK	BJH	HK
siliceous MCM-41	4.0	4.6	2.8	3.7	1.8	0.9
v-gr-MCM-41	4.0	4.6	2.3	3.3	2.3	1.3
brominated v-gr-MCM-41	4.0	4.6	2.1	2.9	2.5	1.7
v-MCM-41L	3.5	4.0	2.2	2.9	1.8	1.1
brominated v-MCM-41L	3.5	4.0	1.8	2.4	2.2	1.6
v-MCM-41H	3.3	3.8	1.5	2.1	2.3	1.7
brominated v-MCM-41H	3.3	3.8	1.2	1.7	2.6	2.1
LP-v-MCM-41	5.7	6.6	3.8	5.8	2.8	0.8

^a $a_0 = 2d_{100}/\sqrt{3}$ for these hexagonal structures.

**Figure 9.** Nitrogen adsorption-desorption isotherm of LP-v-MCM-41. The inset shows the corresponding BJH pore size distribution.**Figure 10.** $\log I$ vs $\log q$ SANS plots for (□) siliceous MCM-41 and (●) v-MCM-41L, both saturated with a 66% D₂O/34% H₂O solution.

absorption at $\lambda_{\max} = 412$ nm during bromination in dichloromethane for three vinyl-modified MCM-41 samples with different pore diameters. The three samples, v-gr-MCM-41, v-MCM-41L, and LP-v-MCM-41, had comparable loadings of vinyl groups, based on the vinyl content of the initial reaction mixtures or on the bromine content of the completely brominated products. The pore sizes calculated from the BJH method were 2.3 nm for v-gr-MCM-41, 2.2 nm for v-MCM-41L, and 3.8 nm for LP-v-MCM-41. The absorbance values of all vinyl-modified MCM-41 samples dropped quickly during the first 5 min, suggesting that reactions occurred on the external surfaces of those samples. As expected, the reaction rate of the larger pore

**Figure 11.** Plot of relative absorbance of Br₂/CH₂Cl₂ solutions ($\lambda_{\max} = 412$ nm) vs time of stirring above vinyl-functionalized MCM-41 samples: (○) v-MCM-41L, (□) LP-v-MCM-41, and (◆) v-gr-MCM-41.**Figure 12.** Plot of relative absorbance of bromine solutions vs time of stirring above v-MCM-41L: (●) solvent CH₂Cl₂ ($\lambda_{\max} = 412$ nm); (□) solvent CCl₄ ($\lambda_{\max} = 416$ nm).

sample, LP-v-MCM-41, was ca. 1.9 times faster than that of v-MCM-41L during the first 340 min. This pore size dependence of bromination provided evidence that limited diffusion was one of the factors controlling the reaction rate.

The solvent also contributed to the reaction rate. Figure 12 shows a comparison of bromination rates for reactions carried out with dichloromethane and carbon tetrachloride as solvents. For both solvents, an initial rapid decrease in relative intensity of the bromine absorption was observed. To determine whether this intensity decrease was caused simply by adsorption of

bromine molecules on the high surface area support, a control experiment was carried out with siliceous MCM-41 in dichloromethane. In that experiment the measured absorbance at $\lambda_{\text{max}} = 412$ nm remained constant over a period of 20 min. Thus, the initial absorbance decrease observed for the vinyl-modified samples is believed to arise only from the bromination of vinyl groups, most likely at the easily accessible external surface.

At the initial stage, the reaction rate was virtually identical in both solvents. However, after 40 min, the reaction was approximately 2.3 times faster in dichloromethane than in carbon tetrachloride. The difference in the reaction rates was attributed to the differences in molecular sizes, molecular weights, and polarities of the two solvents. Bromination of olefins is known to occur via a 1:1 olefin bromine π -complex, which is normally followed by rapid production of bromonium–bromide ion pairs.⁴³ These processes display various degrees of reversibility.⁴⁵ The solid vinyl–MCM-41 support may stabilize the intermediate π -complex, similar to observations made with bulky olefins.⁴⁶ In addition, a low-polarity solvent, such as carbon tetrachloride, is less efficient at assisting the ion pair formation. Thus, it may favor the 1:1 π -complex in the equilibrium between the complex and the bromonium ion.

To minimize solvent effects, a gas-phase bromination was carried out on dried vinyl-modified MCM-41 samples. On the basis of a ^{13}C CP MAS NMR spectrum, the gas-phase bromination was complete within 40 min. The results suggest that hindered diffusion of Br_2 is not the exclusive reason for the slow reaction in solution but that solvent molecules must also contribute to the observed kinetic effects.

On the basis of these observations, we propose that vinyl groups line the walls throughout the channels, but groups on the external particle surface or near the channel openings are brominated first. They can cause some hindrance for additional Br_2 molecules through steric effects, induced dipole interactions, and weak charge transfer interactions. Solvent molecules present in the channels are likely to contribute to the hindered diffusion of Br_2 . The rate deceleration may therefore be attributed not only to a decrease in the bromine concentration with time but also to slower diffusion rates as the number of dibromoethyl sites increases and the effective pore space decreases.

It was notable that the grafted sample, v-gr-MCM-41, reacted almost completely within 220 min (Figure 11); i.e., its bromination rate was significantly faster than for the other two samples, even though it had only a slightly larger pore diameter than v-MCM-41L and much smaller pores than LP-v-MCM-41. To elucidate this phenomenon, one needs to consider differences in surface connectivity of vinyl groups for grafted and directly synthesized materials, as well as differences in surface group distributions. In the case of v-gr-MCM-41, vinylsilanes are anchored to surface silanol groups of siliceous MCM-41. With an additional $-\text{O}-\text{Si}-\text{O}-$

unit between the silica wall and the vinyl groups, grafted vinylsilane groups protrude further away from the wall surface than the tightly bound vinyl groups incorporated by co-condensation (see above). According to simple molecular mechanics calculations (MM2) with the CS Chem 3D Pro program suite,³⁸ the estimated distances between the vinyl carbon next to the silicon atom and the MCM-41 wall surface are approximately 1.9 and 4.5 Å for products from the direct synthesis and the grafting procedure (singly bound to the wall surface), respectively. The grafted vinyl groups are thus more liable to attack by bromine molecules because of less steric hindrance between the vinyl groups and the wall of MCM-41, and as a result, a faster reaction rate is expected if other conditions are identical. However, one should keep in mind that in Figure 11 all three samples exhibited a fast initial decrease in absorbance due to reaction with easily accessible surface groups. This observation implies that the reaction rate cannot be totally attributed to the connectivity of vinyl groups. Instead, it suggests a difference in distributions of vinyl groups. It appears that in v-gr-MCM-41 vinyl groups are mostly concentrated on the external surfaces and on internal surfaces close to the pore windows, whereas direct co-condensation results in an even distribution of organic groups throughout the internal and external surfaces of the sample. A predominance of organic functional groups on the external surface of grafted MCM-41 samples has also been observed by Shephard et al.¹³

The difference in the distribution of functional groups was supported by XPS measurements. The escape depth of electrons in XPS is a few nanometers; therefore, this technique emphasizes the external surface contributions of the particles, which have dimensions on the order of micrometers. The bromine content of fully brominated vinyl–MCM samples was determined by XPS and compared with values determined by bulk chemical analysis, which take into account the whole sample. The ratio of bromine in the grafted sample to bromine in the sample from direct synthesis ($[\text{Br}]_{\text{grafted}}/[\text{Br}]_{\text{direct}}$) was 1.03 for the bulk chemical analysis and 1.24 for the XPS data, indicating that for the grafted sample more bromine and hence more vinyl groups were present within a few nanometers of the surface and that the deeper parts of the channels were probably less functionalized.

Thermal and Hydrothermal Stability. The thermal stability of the organic functional groups within the mesoporous materials (v-MCM-41L and its brominated sample) was determined by thermogravimetric analysis (Figure 13). After initial loss of solvent, the removal of the vinyl or dibromoethyl groups commenced at 280–290 °C and continued up to 440 or 520 °C, respectively. An additional weight loss occurred at higher temperatures due to further condensation of the silicate walls, as observed in other mesoporous silicates.⁴⁷

Hydrothermal stability is an important issue in many potential applications of porous materials.^{48,49} Conven-

(45) Bellucci, G.; Bianchini, R.; Chiappe, C.; Lenoir, D.; Attar, A. *J. Am. Chem. Soc.* **1995**, *117*, 6243–6248.

(46) Bellucci, G.; Chiappe, C.; Bianchini, R.; Lenoir, D.; Herges, R. *J. Am. Chem. Soc.* **1995**, *117*, 12001–12002.

(47) Steel, A.; Carr, S. W.; Anderson, M. W. *Chem. Mater.* **1995**, *7*, 1829–1832.

(48) Ryoo, R.; Kim, J. M.; Ko, C. H.; Shin, C. H. *J. Phys. Chem.* **1996**, *100*, 17718–17721.

(49) Ryoo, R.; Jun, S. *J. Phys. Chem. B* **1997**, *101*, 317–320.

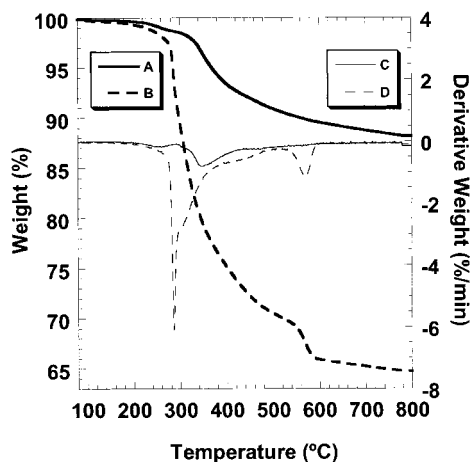


Figure 13. TGA and derivative TG curves of v-MCM-41L after surfactant extraction (A and C, respectively) and brominated v-MCM-41L (B and D, respectively).

tional MCM-41 exhibits high thermal stability,⁵⁰ but its structure is easily degraded in boiling water. Several studies have been directed toward an enhancement of the hydrothermal stability of MCM-41 or other periodic mesoporous materials. Postsynthesis treatment of MCM-41 with TEOS has been shown to increase the hydrothermal stability.⁵¹ Ryoo et al. reported that the hydrothermal stability of MCM-41 can be improved by adding salts, such as KCl, NaCl, or EDTA, to the reaction mixture during the hydrothermal crystallization process.⁴⁹ Recently, Zhao et al. demonstrated that mesoporous materials prepared using nonionic oligomeric surfactants or block copolymer surfactants were stable in boiling water up to 48 h.⁵²

Hydrothermal stability tests were carried out for vinyl-modified MCM-41 samples produced from both the grafting method and the direct synthesis method. Figure 14 presents the PXRD patterns of samples that were hydrothermally treated in boiling DDI water for 24 h. The PXRD intensity and the number of reflections were used to gauge the hydrothermal stability of the samples. The vinyl-grafted sample still exhibited long-range order with three reflections after treatment in boiling water for 24 h. The intensity of the d_{100} reflection decreased by about 30%, and the d_{100} spacing contracted slightly (0.1 nm). In comparison, 1 day treatment of the unprotected host (siliceous MCM-41) in boiling water resulted in a shift of the d_{100} spacing from 4.0 to 3.8 nm with a 66% decrease in intensity and the complete disappearance of higher angle reflections. The higher hydrothermal stability of the sample after grafting was attributed to an enhancement of the wall thickness and to the hydrophobic nature of the vinyl groups, which protected the walls from attack by water. The hydrothermal stability of v-MCM-41H prepared in a one-pot synthesis was lower than that of v-gr-MCM-41. The PXRD intensity decreased by about 60%, and the d_{100} spacing shifted from 3.3 to 3.1 nm after heating in water for 24 h. According to ²⁹Si MAS NMR data (Table 2), v-MCM-41H has a $Q^4/(Q^3 + T^n)$ ratio of 1.0, which is lower than

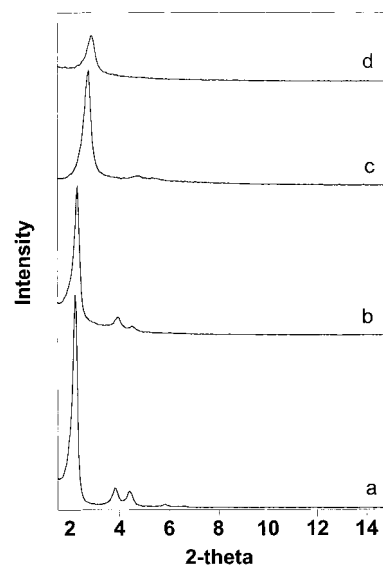


Figure 14. Powder XRD patterns of (a) v-gr-MCM-41, (b) v-gr-MCM-41 after 1 day hydrothermal treatment in boiling water, (c) v-MCM-41H (1 VTMS:2.1 TMOS) after surfactant extraction, and (d) v-MCM-41H after 1 day hydrothermal treatment in boiling water.

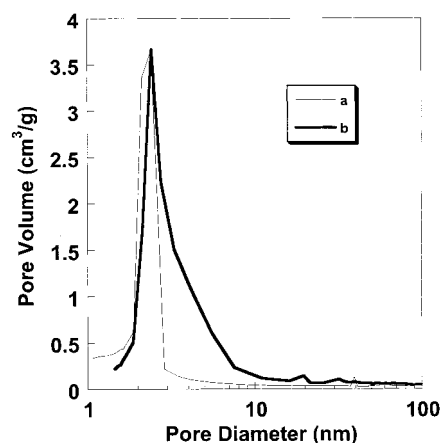


Figure 15. BJH pore size distributions of (a) v-gr-MCM-41 and (b) sample (a) after 1 day hydrothermal treatment in boiling water.

the Q^4/Q^3 ratio (1.8) of siliceous MCM-41. The low $Q^4/(Q^3 + T^n)$ ratio implies a less condensed silica wall structure of v-MCM-41H compared to siliceous MCM-41, as well as the presence of more unprotected Si-OH groups.

Nitrogen adsorption measurements of these samples were performed as an alternative method to judge their hydrothermal stability. After 1 day treatment in boiling water, the surface area (1050 m²/g) of siliceous MCM-41 decreased by 39%, and the pore size distribution broadened compared to the sample before hydrothermal heating. On the other hand, a v-gr-MCM-41 sample that was boiled in H₂O for 1 day exhibited a similar BET surface area (1030 m²/g) and a comparable pore size distribution in the region of 2–3 nm as untreated v-gr-MCM-41 (998 m²/g). However, the pore size distribution in the range of 3–8 nm was broadened (see Figure 15), and the pore volume increased from 0.68 to 1.01 cm³/g. These observations imply that minor structural degradations occurred in the channel walls where vinylsilation had not been carried out. Similar hydrothermal

(50) Chen, C. Y.; Li, H. X.; Davis, M. E. *Microporous Mater.* **1993**, 2, 17–26.

(51) McCullen, S. B.; Vartulli, J. C. U.S. Patent 5156829, 1992.

(52) Zhao, D. Y.; Huo, Q. S.; Feng, J. L.; Chmelka, B. F.; Stucky, G. D. *J. Am. Chem. Soc.* **1998**, 120, 6024–6036.

stability is expected for hybrid MCM-41 samples possessing other hydrophobic organic surface groups.

Absorption of Nonpolar Solvents. Vinyl-modified MCM-41 exhibited interesting sorption properties which were investigated qualitatively at this stage. Because of their hydrophobic surface and the small particle size (a few micrometers), v-MCM-41 particles tended to float on the surface of water. However, when v-MCM-41 was shaken with a mixture of chloroform and water, the solids sank to the bottom of the flask as they absorbed the denser organic solvent. In mixtures of toluene and water (phase separated or as emulsions), toluene was absorbed by v-MCM-41, and the filled solids tended to form clumps. On the basis of their affinity for nonpolar solvents, vinyl-MCM-41 and related materials may be useful for removing small amounts of organic fractions from water or for carrying out “dry” chemical reactions within the channels. More detailed quantification of the sorption properties of these hybrid mesoporous sieves will be carried out in future studies.

Conclusion

Vinyl-functionalized MCM-41 samples were prepared by a postsynthesis grafting process and by a direct co-condensation synthesis. In direct syntheses of v-MCM-41 samples, hexagonally ordered products with higher loadings of vinyl groups were obtained by using methoxy-based precursors (1 VTMS:2.1 TMOS) rather than ethoxy-based precursors (1 VTES:4 TEOS), most likely due to the faster hydrolysis and condensation rates of the former. Vinyl-grafted MCM-41 samples exhibited higher hydrothermal stability than conventional MCM-41 samples due to the increases of channel wall thickness or/and hydrophobic effects that may minimize degradation of the framework by hydrolysis.

The most critical differences between vinyl-grafted MCM-41 prepared by the present PSG process and vinyl-MCM-41 samples produced from the direct synthesis appear to be the mode of surface attachment and

the location of the majority of vinyl groups. On the basis of the nitrogen adsorption experiments and the kinetic study of bromination, we believe that most vinyl groups in a grafted sample are located on external surfaces and internal surfaces close to the pore windows. This implies that vinyl groups are not uniformly distributed through the MCM-41 channel surfaces in these samples. On the other hand, vinyl MCM-41 produced from the direct synthesis method contained uniformly distributed vinyl groups within mesopore channels, based on several experiments, including PXRD, XPS, the kinetic study of bromination, and the analysis of weight-corrected pore volumes and surface areas before and after bromination.

Each of the two functionalization methods has certain advantages. If uniform surface coverage with organic groups is desired in a reliable synthesis, the direct method may be the better choice. However, samples from the PSG method are structurally better defined and more hydrothermally stable than samples from the direct synthesis method. Furthermore, pore size control is relatively straightforward because organic functionalization takes place in premade host samples.

Acknowledgment. This work was supported by 3M, Dupont, the David and Lucille Packard Foundation, and the National Science Foundation (DMR-9701507). M.H.L. gratefully acknowledges the Center for Interfacial Engineering at the University of Minnesota for a CIE-NSF graduate fellowship. This work has benefited from the use of the Intense Pulsed Neutron Source at Argonne National Laboratory. This facility is funded by the U.S. Department of Energy, BES-Materials Science, under Contract W-31-109-Eng-38. The authors acknowledge P. Thiyagarajan (IPNS) for assistance with the SANS experiment and C. F. Blanford for the electron microscopy data.

CM990369R